Femtosecond Excited State Studies of the Two-Center Three-Electron Bond Driven Twisted Internal Charge Transfer Dynamics in 1,8-Bis(dimethylamino)naphthalene

Grzegorz Balkowski,[†] Anna Szemik-Hojniak,[‡] Ivo H. M. van Stokkum,[§] Hong Zhang,*[,†] and Wybren J. Buma*[,†]

Van't Hoff Institute for Molecular Sciences, Faculty of Science, University of Amsterdam, Nieuwe Achtergracht 127-129, 1018 WV Amsterdam, The Netherlands, Faculty of Chemistry, Wrocław University, 14 Joliot-Curie Street, 50-383 Wrocław, Poland, and Department of Physics and Astronomy, Free University, Amsterdam, The Netherlands

Received: January 24, 2005; In Final Form: February 25, 2005

Femtosecond fluorescence upconversion and transient absorption experiments have been performed to monitor the photoinduced electronic, geometry, and solvent relaxation dynamics of 1,8-bis(dimethylamino)naphthalene dissolved in methylcyclohexane or *n*-hexane, *n*-dodecane, dichloromethane, and acetonitrile. The data have been analyzed by using a sequential global analysis method that gives rise to species associated difference spectra. The spectral features in these spectra and their dynamic behavior enable us to associate them with specific processes occurring in the molecule. The experiments show that the internal charge-transfer $l\pi^*$ state is populated after internal conversion from the ^1L_a state. In the $l\pi^*$ state the molecule is concluded to be subject to a large-amplitude motion, thereby confirming our previous predictions that internal charge transfer in this state is accompanied by the formation of a two-center three-electron bond between the two nitrogen atoms. Solvent relaxation and vibrational cooling in the $l\pi^*$ state cannot be separated in polar solvents, but in apolar solvents a distinct vibrational cooling process in the $l\pi^*$ state is discerned. The spectral and dynamic characteristics of the final species created in the experiments are shown to correspond well with what has been determined before for the relaxed emissive $l\pi^*$ state.

I. Introduction

The target molecule, 1,8-bis(dimethylamino)naphthalene (Figure 1), henceforth indicated as DMAN, has attracted attention in various fields since its first synthesis by Alder,[1] initially due to its unusual physical properties, and subsequently because of applications such as auxiliary bases in different organic syntheses,[2−4] or gene therapy.[5,6] Early experiments showed that the molecule exhibits an extremely high basicity[7]—a few orders of magnitude more than most of the aromatic amines—and the molecule quite soon became the primary example of a new class of organic "proton sponges", bicenter nitrogen bases that combine a strong basicity with a low nucleophilic character. The exceptional basicity of DMAN as well as its geometrical structure were found to be predominantly determined by the interactions between two nearby dimethylamino groups, i.e., steric strain in competition with resonance and repulsive interactions between the nitrogen lone pairs.[8]

Spectroscopic studies in the gas and solution phase have made clear that the very same interactions also determine to a large extent the spectroscopic properties of the molecule. Fluorescence excitation and dispersed emission studies performed on DMAN seeded in supersonic expansions showed the presence of two species in the ground state, which were assigned to two different conformations of the molecule on the basis of ab initio calculations at the HF/6-31G* level.[9] These studies were recently

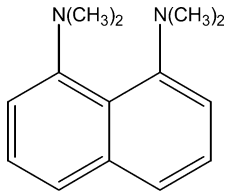

Figure 1. Structure of 1,8-bis(dimethylamino)naphthalene.

complemented by experimental and theoretical studies of the photophysical properties of the molecule in solution.[10] Whereas similar compounds containing only one amino group (e.g. 1-dimethylaminonaphthalenes) have the ^1L_a state as their lowest excited state,[11] we showed that the emissive state in DMAN is a highly polar $l\pi^*$ state with a large internal charge transfer (ICT) character. Ab initio calculations demonstrated that the steric strain and lone pair repulsion accompanying the introduction of the second dimethylamino group in DMAN are primarily responsible for this difference in ordering.[10] The solution studies showed that the emission spectrum exhibits a large Stokes shift even in nonpolar solvents. Since in these solvents stabilization of a polar ICT state by solute−solvent interactions is minor, it was concluded that the molecular structure changes considerably upon excitation to the emissive state. Ab initio calculations and nanosecond transient absorption experiments strongly suggested that this geometry relaxation predominantly involves twisting of the dimethylamino groups, even to such an extent that a complete decoupling occurs of the dimethylamino lone pair orbitals from the naphthalene π-system.[10]

Naively, one might draw parallels with the phenomena that occur in the ICT states of other aromatic amines, in particular with the twisted ICT (TICT) model postulated by Grabowski

* To whom correspondence should be addressed. E-mail: wybren@science.uva.nl. Phone: +31-20-525 6973/6421. Fax: +31-20-525 6456/6422.
[†] University of Amsterdam.
[‡] Wrocław University.
[§] Free University.

10.1021/jp050404j CCC: $30.25
Published on Web 04/02/2005

et al. some 30 years ago.[12] In this model ICT is accompanied by a twisting motion of the amino group from a planar configuration in the locally excited state to an electronically decoupled perpendicular geometry in the ICT state. Recently, however, we have shown that the geometry relaxation process in DMAN has a fundamentally different origin from what is proposed in TICT.[13] In DMAN the driving force for relaxation along the twisting motion can unambiguously be identified as the formation of a two-center three-electron bond between the two nitrogen atoms, in TICT the driving force is associated with the reduction of repulsive interactions between the two unpaired electrons, combined with the stabilization of the highly polar state in polar solvents by solute−solvent interactions.

Despite the wealth of information that has come forward from the solution and quantum chemical studies, there are still several key issues that need to be addressed. One question concerns, for example, how the emissive $l\pi^*$ state is populated. Previously, we have postulated from steady-state absorption and emission spectra that vertical excitation occurs to the ^1L_a state after which internal conversion takes place to the $l\pi^*$ state. Real-time observation of this process would enable us to confirm this conclusion and establish thereby implicitly the order of the lower excited singlet states, and, equally important, allow us to determine the properties of the absorbing ^1L_a state and study the internal conversion process. Similarly, real-time observation of the nuclear conformational changes accompanying the charge-transfer process would provide direct proof of the structural mechanism proposed for the process, and provide the means to investigate the role of intermolecular interactions and vibrational relaxation dynamics.

In the present paper we have applied femtosecond transient absorption and fluorescence upconversion spectroscopy to monitor the dynamic processes—with an emphasis on the charge transfer and excitation relaxation dynamics in the electronic excited states—of DMAN in real time. Although the fluorescence upconversion experiments provide some insight into the initial dynamics, it turns out that the most complete picture is provided by transient absorption spectroscopy. The complex transient absorption spectra have been disentangled by a global analysis in combination with a target analysis, which yielded species associated difference spectra (SADS). From the analysis of the spectral features present in the SADS and the dynamic behavior of SADS, the specific processes discussed above could clearly be identified and investigated, i.e., internal conversion of the initially excited ^1L_a state to the unrelaxed $l\pi^*$ state (below 300 fs in all solvents), twisting motion of the dimethylamino groups (up to 1 ps in acetonitrile and dichloromethane), vibronic cooling (6 to 15 ps, observed only in apolar solvents), and decay of the relaxed $l\pi^*$ state to the ground state (ranging from 50 ps in acetonitrile to nanosecond time scale in methylcyclohexane and *n*-dodecane).

II. Experimental Section

1,8-Bis(dimethylamino)naphthalene (DMAN) was purchased from Aldrich and used without further purification. The solvents employed (methylcyclohexane or *n*-hexane, *n*-dodecane, dichloromethane, and acetonitrile) were of spectroscopic grade when purchased from Aldrich. Methylcyclohexane, *n*-hexane, and *n*-dodecane were used as received, and dichloromethane and acetonitrile were dried over type 3A molecular sieves prior to use. Steady-state absorption and fluorescence spectra were recorded on Cary 3 (Varian) and Spex Fluorolog 3 spectrometers, respectively.

The setup used for the femtosecond transient absorption experiments has been described in detail before.[14] Briefly, a 130 fs (fwhm) pulse train at 800 nm with a repetition rate of 1 kHz is generated by a Spectra Physics Hurricane regenerative amplifier laser system. This pulse train is separated into two parts. One part pumps an Spectra Physics OPA 800 system to provide excitation pulses—in the present case at 330 nm—the other part is focused on a calcium fluoride crystal to generate a white light continuum from 350 to 800 nm that is used for the probe pulse. The total instrumental response is about 200 fs (fwhm). In the present experiments magic angle conditions were used for the pump and probe beam. Experiments were performed at ambient temperature on solutions with an optical density of ca. 0.5 in a 1 mm cell. To avoid effects resulting from the high transient power radiation, the excitation power was kept as low as $\sim 5\ \mu$J per pulse and a pump spot diameter of about 1 mm was used. Apart from lowering the excitation intensity, the influence of thermal effects and possible photodegradation of the sample was taken care of by placing the circular cuvette containing the solution in a homemade rotating ball bearing (1000 rpm). Absorption and emission spectra taken before and after the experiments were under these conditions indeed identical.

Femtosecond upconversion experiments have been performed with the setup described extensively in ref15. In this setup a diode-pumped CW Nd:YVO_4 laser (Spectra Physics, Millennia X) pumps a Ti:sapphire laser (Spectra Physics, Tsunami), providing 60 fs pulses at 800 nm at a repetition rate of 82 MHz. These pulses are amplified in a regenerative amplifier laser system (Quantronix) to about 460 μJ at a repetition rate of 1 kHz, and subsequently split into two beams. One of the beams serves to pump an optical parametric amplifier system (TOPAS Light Conversion Ltd.) that provides wavelength-tunable pulses to excite the sample, and the other beam serves as the gating beam for the fluorescence. The system response time of this setup as measured from the cross-correlation signal of the excitation and gating pulses is estimated to be approximately 280 fs (fwhm). Experiments have been performed under magic angle conditions for pump and gating beams on solutions in a quartz cell of 1 mm thickness. The cell was attached to a sample holder that was driven electrically back and forth perpendicular to the excitation beam to prevent heating of the sample.

III. Results and Discussion

The steady-state absorption and emission spectra of DMAN in *n*-hexane are shown in Figure 2. The absorption spectra in the solvents employed in the present experiments are essentially the same and all show a lowest absorption band that peaks around 330 nm. TD-DFT calculations[10,13] show that this band is associated with the ^1L_a state. The emission spectrum, on the other hand, is quite sensitive to the polarity of the solvent as has been described in detail before.[10] Due to the large change in dipole moment upon excitation to the emissive $l\pi^*$ ICT state (9.3 D compared with 1.12 D in S_0[16]), the emission shifts substantially to the red with increasing polarity. The large Stokes shift observed already in an apolar environment, where stabilization of the ICT state by solvent molecules is only minor, has been attributed to geometry reorganization mainly connected with the twisting motion of the dimethylamino groups (vide supra).

Our goal is to probe these internal conversion as well as geometry and energy relaxation processes directly by applying femtosecond transient absorption and fluorescence upconversion spectroscopy. As an aide in understanding and distinguishing the observed processes, we have varied the environmental conditions of the probe molecules, i.e., polarity and viscosity,

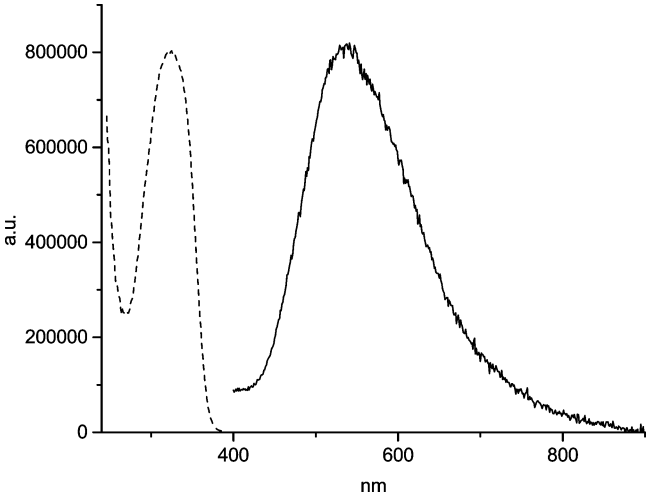

Figure 2. The absorption (dotted line) and fluorescence (solid line) spectra of DMAN in *n*-hexane. The fluorescence spectrum has been obtained for excitation at 330 nm.

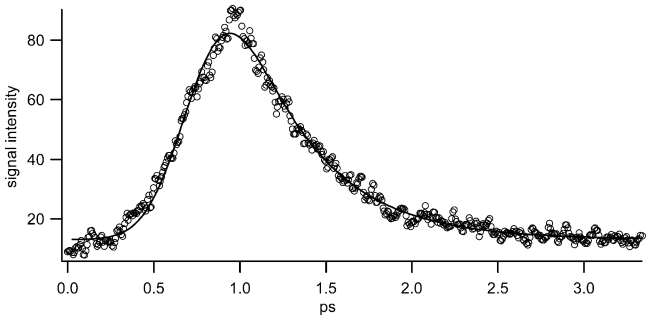

Figure 3. The femtosecond upconversion decay trace of DMAN in *n*-hexane probed at an emission wavelength of 520 nm. The solid line is a fit to a biexponential decay with a dominant (>90%) contribution from a 0.3 ps decay.

by performing measurements in methylcyclohexane (or in some cases *n*-hexane[17]), *n*-dodecane, dichloromethane, and acetonitrile. The transient absorption measurements were done for each solution in three separate time windows of 10, 100, and 1000 ps. In the femtosecond upconversion experiments the same solvents have been employed,[17] but for acetonitrile solutions it was found that the signal intensity was too low to obtain useful decay traces.

Figure 3 shows a femtosecond upconversion transient obtained for DMAN dissolved in *n*-hexane excited at 330 nm and detected at 520 nm, i.e., close to the steady-state emission maximum. Transients that are qualitatively similar were observed at other detection wavelengths and also for DMAN dissolved in other solvents. Fitting of these transients reveals that they are dominated by a decay on the subpicosecond time scale, but definitely also require contributions from decays at longer ((sub)nanosecond) time scales. Comparison of these latter contributions show that, qualitatively speaking, they are larger for longer detection wavelengths. Despite the small amplitude(s), the spectral characteristics of the other components are responsible for the appearance of the steady-state emission spectrum because of the considerably longer lifetime(s). From the femtosecond upconversion transients we can thus draw the important conclusion that after excitation of DMAN an ultrafast process occurs that changes dramatically the radiative properties of the emissive state. The transient absorption results discussed below will show that this ultrafast process is associated with the twisting of the dimethylamino groups.

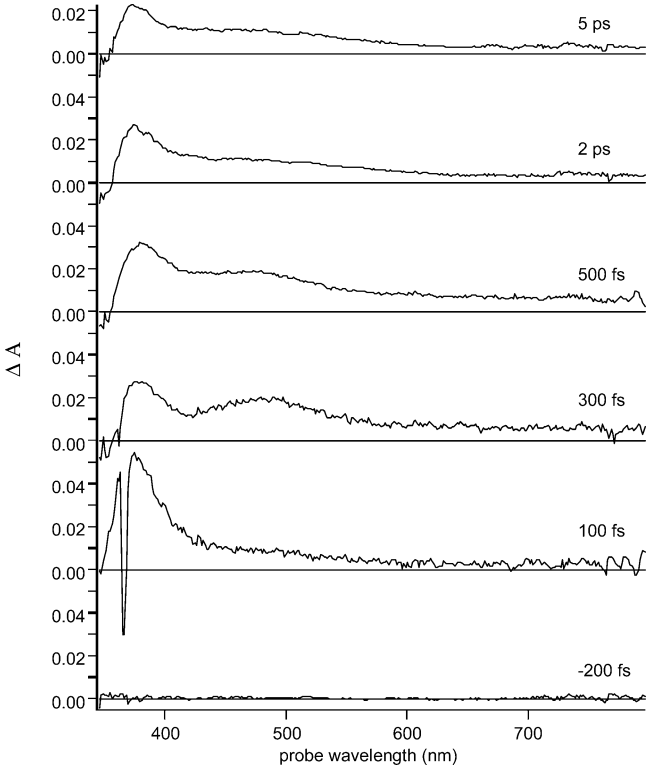

Figure 4. Transient absorption spectra of DMAN in *n*-dodecane at various delay times (−0.2 to 5 ps) after excitation at 330 nm.

Transient absorption spectroscopy turns out to elucidate the relevant dynamical processes further. In the frequency domain, we obtain typically spectra such as the ones displayed in Figure 4 for DMAN in *n*-dodecane. The absorption spectrum consists initially of one broad band with a distinct maximum at ∼380 nm that decays quickly (<1 ps), after which a spectrum is formed that can be described as the sum of two bands around 380 and 500 nm. Of particular interest is the observation that for short delay times an emissive feature is present around 420 nm. The decay traces shown in Figure 5a for a number of selected probe wavelengths in the time domain provide an alternative view on these dynamics. From these traces it is directly evident that the decay dynamics are rather complex and that an accurate description in terms of exponential decays involves at least three or more contributions. Qualitatively speaking, we observe at the blue side of the transient absorption spectrum an ultrafast decay of the signal followed by an in-growth and subsequent decay on the picosecond and ultimately nanosecond time scales. The contribution of this ultrafast decay becomes increasingly smaller for longer probe wavelengths where, apart from a subpicosecond rise, an additional in-growth on the picosecond time scale occurs, followed by picosecond and nanosecond decays.

Similar observations can be made for the transient absorption spectra in the other solvents, albeit that the signal-to-noise ratio in those spectra was noticeably poorer than that obtained for *n*-dodecane solutions, as can, for example, be observed in Figure 5b, where transient absorption decay traces of DMAN in methylcyclohexane are shown. Figures 4 and 5 indicate that the excited-state absorptions in DMAN are small in a large part of the probe region accessible in the present experiments. Moreover, the kinetic curves were found to be strongly probe-wavelength dependent and at some wavelengths rather complex. These factors made it difficult to interpret the experimental data reliably by fitting decay curves at only a limited number of different wavelengths. Global analysis of the transient absorption

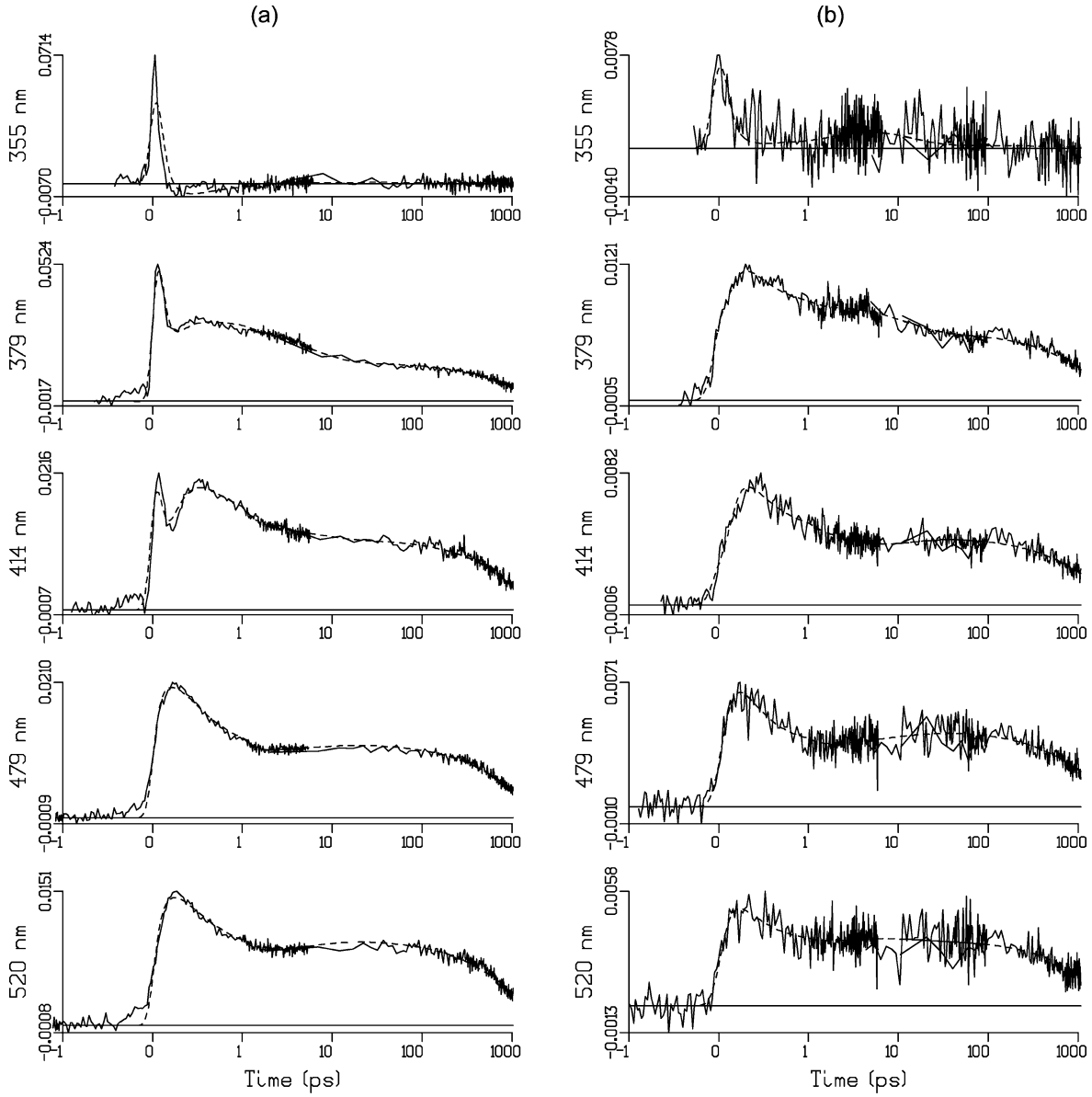

Figure 5. Decay traces of the transient absorption signal of DMAN in (a) *n*-dodecane and (b) methylcyclohexane for various probe wavelengths. Dashed lines indicate the fit described in the text. Note that the time axis is linear from −1 ps to 1 ps relative to the maximum of the IRF, and logarithmic afterward.

spectra at all investigated probe wavelengths and in all time windows did, however, lead to a consistent picture. More specifically, we employed a sequential global analysis method[18,19] in which the excited species assumed to be present at time zero evolves into another species with a certain decay rate k_1. This species subsequently evolves with rate k_2 into a third species and so on. The last species n obviously decays to the ground state of the molecule. Associated with each species is its own spectrum, the species associated difference spectrum (SADS), $A_i(\lambda)$. The isotropic decay $I_{iso}(\lambda,t)$ is then described by:

$$I_{iso}(\lambda,t) = [\sum_{i=1}^{n} A_i(\lambda)c_i(t)] \otimes I(t)$$

where $I(t)$ is the instrument response and $\otimes$ denotes convolution. The concentrations $c_i(t)$ are exponential functions of the decay rates k_1, k_2, ..., k_n. In this model no back reaction or branching is taken into account. For the dynamic processes such as internal conversion and large amplitude motions that we consider here substantial branching or back reactions are indeed not expected as the energy differences between the states involved are too large and because they are unidirectional.

Global analysis of the data reveals that they can be fitted satisfactorily with a model consisting of five species in the case of *n*-dodecane, four for methylcyclohexane, while only three species need to be employed for the polar solvents methylcyclohexane and acetonitrile. The SADS and the decay rates obtained from these analyses are given in Figure 6 and Table 1, respectively. If we ignore for the moment SADS ι that only appears for *n*-dodecane, we observe from Figure 6 that with the present instrumental response an initial species φ is formed upon photoexcitation that has a similar absorption spectrum in all solvents, consisting of a broad absorption band in the 350−600 nm region with a narrow emissive band in the 410−420 nm region. The latter band can nicely be fitted to a Gaussian with the parameters given in Table 2.

Our previous experimental and theoretical results implied that excitation of DMAN at 330 nm populates the ^1L_a state.[10,13] The same calculations showed that the Stokes shift for the emission from the ^1L_a state should be considerably smaller than that for

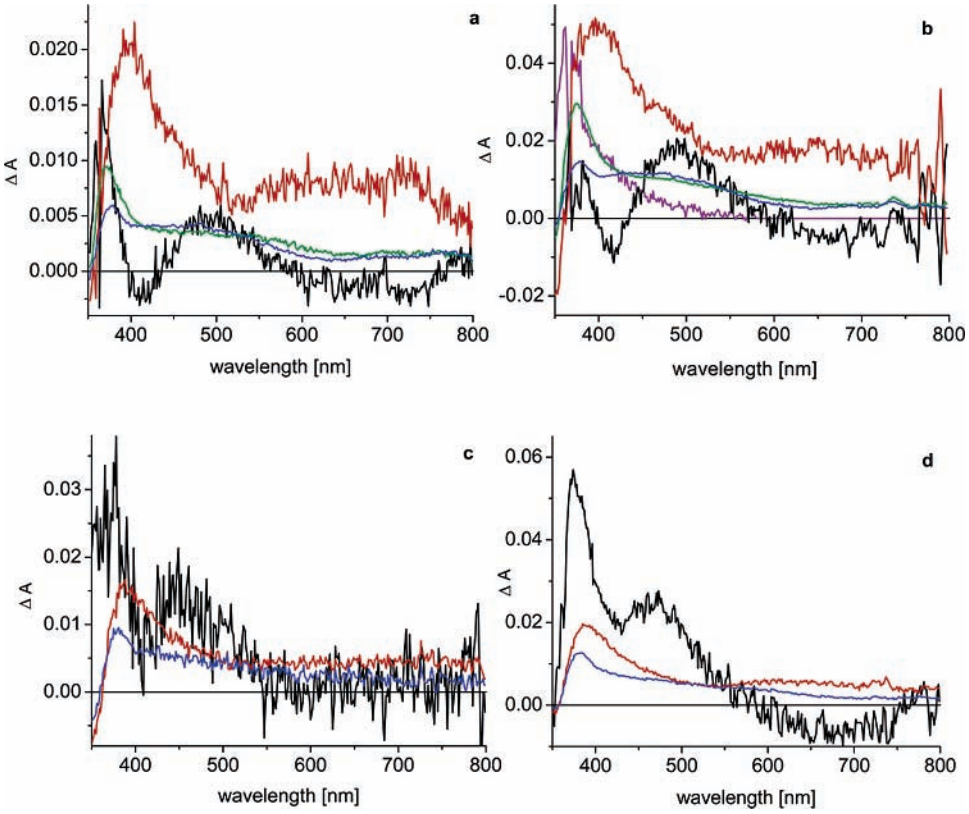

Figure 6. Species associated difference spectra (SADS) of DMAN solution in (a) methylcyclohexane, (b) *n*-dodecane, (c) dichloromethane, and (d) acetonitrile obtained from a sequential target analysis involving species ι (purple) → φ (black) → κ (red) → λ (blue) → μ (green) for *n*-dodecane, φ (black) → κ (red) → λ (blue) → m (green) for methylcyclohexane, and φ (black) → κ (red) → μ (green) for dichloromethane and acetonitrile. The amplitude of trace ι (purple) in *n*-dodecane has been divided by a factor of 4. The spike-like feature near 365 nm observed in φ (black) for methylcyclohexane and ι (purple) for *n*-dodecane is associated with Raman scattering from the solvent.

TABLE 1: Lifetimes (ps) of the Components of the SADS Observed for DMAN in Various Solvents[a]

	methylcyclohexane	*n*-dodecane	dichloromethane	acetonitrile
ι		0.07		
φ	0.3	0.3	0.3	0.06
κ	0.3	0.3	1.0	0.9
λ	14.7	5.6		
μ	1435	1068	168	54

[a] Errors (1σ) are estimated to be 10% (30%) for values above (below) 1 ps.

TABLE 2: Gaussian Fit Parameters of the Emissive Band in SADS φ in Various Solvents

solvent	center (cm^{-1})	width (cm^{-1})
methylcyclohexane	24500 ± 300	4800 ± 1900
n-dodecane	24360 ± 130	4100 ± 400
dichloromethane[a]		
acetonitrile	23950 ± 190	4200 ± 1400

[a] Band could not be fitted reliably.

the $l\pi^*$ state and less solvent dependent because the dipole moment of the ^1L_a state is similar to that of the ground state.[13] The SADS φ observed here provide a direct and straightforward verification of these predictions: the stimulated emission band around 410−420 nm is right where emission from the ^1L_a state is expected to occur, while the observed dependence of the emission maximum on the polarity of the solvent is consistent with a small change in dipole moment upon excitation.[20]

In *n*-dodecane the global analysis results indicate that species φ is not the initial species that can be detected but that it is formed from another species ι that decays on a sub-100 fs time scale. In view of the discussion above, we associate this species with the Franck−Condon excited ^1L_a state, which populates the relaxed ^1L_a state via intramolecular vibrational relaxation (IVR). The fact that we can observe this process in *n*-dodecane does not imply that it is not present in the other solvents; in fact, the traces at 355, and to a lesser extent at 379 and 414 nm, in Figure 5b indicate the presence of a similar ultrafast process in methylcyclohexane, but the signal-to-noise ratio precludes a reliable determination of the SADS and the associated decay rate.

The decay time of the ^1L_a state varies from 0.06 ps in acetonitrile to 0.3 ps in methylcyclohexane, *n*-dodecane, and dichloromethane. Species that are formed from the decay of the ^1L_a state all exhibit SADS in which the stimulated emission feature around 410−420 nm is absent. This is an unambiguous indication that another electronic state is formed, and we thus associate the decay of the initial species with the internal conversion from the ^1L_a state to the unrelaxed $l\pi^*$ state. The latter state has entirely different emissive properties. First, emission from the $l\pi^*$ state occurs far more to the red (vide supra); second, the oscillator strength of the transition from this state to the ground state is at least 10 times smaller.[10,21] In many organic molecules the internal conversion process proceeds on a time scale much shorter than any vibrational relaxation time[22] and is often found to be ultrafast (less than picoseconds). For example, for various bridged and unbridged luminescent styrile dyes the typical IC time was found in the range up to 300 fs[23] with essentially no influence of the energy gap between the S_2 and S_1 states on the rate constant. The same conclusion is now drawn from the present results on DMAN, where the energy gap between the quasidegenerate excited states involved is even much smaller.

The excited-state absorption spectrum of the unrelaxed $l\pi^*$ state is represented by the SADS κ in Figure 6. The spectrum

of this component consists of a broad absorption with a distinct maximum around 400 nm and extends to ca. 600 nm, with possibly an unresolved shoulder at about 500 nm. To assign the process associated with its decay and identify the species that is formed, we first notice that subsequent SADS exhibit essentially the same characteristics as SADS κ, albeit that the excited-state absorption around 400 nm shifts to the blue and sharpens up. These features indicate that we are observing relaxation processes that take place in one and the same electronic state. Furthermore, we recall that previous work showed that geometry relaxation of the molecule—involving mainly twisting of the dimethylamino groups—was crucial to understand the large Stokes shift observed already in apolar solvents.[10] In its electronic ground state the molecule adopts an equilibrium conformation in which the dimethylamino groups are twisted with an angle of about 42°. This geometry is far from optimal for either of the lower two excited ^1L_a and $l\pi^*$ states. In the ^1L_a state the molecule adopts a partially untwisted configuration, and for the $l\pi^*$ state the formation of a two-center three-electron bond twists the dimethylamino groups to maximize the overlap between the lone pair orbitals.

After internal conversion from the photoexcited ^1L_a state the molecule will thus find itself in the $l\pi^*$ state in a conformation that is far from optimal and will be subject to geometry relaxation. The process associated with the decay of SADS κ is therefore assigned to the twisting motion of the dimethylamino groups. Because of the large-amplitude motion character of the twisting process, one might hope to find further support for this conclusion by considering the influence of the viscosity on the decay time, i.e., when comparing two solvents of about the same polarity, one expects the decay time to increase for the more viscous solvent. The accuracy with which the decay time can be determined in methylcyclohexane and *n*-dodecane does not allow us to make such a reliable comparison; for both solvents a decay time of about 0.3 ps is found. For the polar solvents dichloromethane and acetonitrile a different situation is encountered; here values are obtained of 0.9 ps for acetonitrile and 1.0 ps for dichloromethane, which are comparable with the diffusive solvent reorganization times.[24]

For a polar solute molecule dissolved in polar solvents the solvation dynamics is often found to play a critical role in the excitation relaxation processes.[25] Hynes et al. proposed a two-dimensional reaction approach to explain the dynamics of TICT processes in polar solvents.[26] In this approach both twisting and solvation are taken into account. As can be expected, the reaction path on the potential energy surface constituted by the twisting and solvent coordinates does in general not show pure twisting or solvation character, albeit that in some extreme cases one of the two might appear to be dominating. Whether the kinetics of the process show viscosity or solvation dependence relies on the twisting motions being "slow" or "fast" with respect to the solvation.[27,28] For Michler's ketone in alcoholic solvents, for example, the "slow" solvation limit was reached.[29] This approach was also applied to explain the spectroscopic behavior of DMAN-like molecules such as 4-(9-anthranyl)-*N*,*N*′-dimethylaniline.[30] For DMAN in polar solvents we find in the present study that the reaction and solvent reorganization times are comparable, i.e., we have to conclude that the solvation dynamics is dominant in the TICT process.

The SADS λ is only observed for the apolar solvents methylcyclohexane and *n*-dodecane. It exhibits a narrow excited-state absorption around 380 nm, superimposed on a broad background that extends up to beyond 600 nm. The decay time of this species is 15 ps in methylcyclohexane and 6 ps in *n*-dodecane. Since the reorganization energy associated with geometry relaxation of the $l\pi^*$ state is quite large, the DMAN molecule still has a considerable amount of energy stored in the vibrational degrees of freedom after internal conversion and twisting of the dimethylamino groups. Dissipation of this energy to the surrounding solvent molecules occurs via vibrational cooling on the picosecond time range.[31−36] The species that is associated with the SADS λ is therefore most logically associated with the vibrationally hot $l\pi^*$ state, and the decay process with vibrational cooling. One might argue that in the SADS λ and μ the difference in the width of the band around 380 nm is minimal. For large molecules the cooling process often involves many vibrational modes as opposed to a few modes in small molecules. As a result, the shape of the spectrum, which reflects the vibrational population density, does not show significant changes upon vibrational cooling. Similar observations have been made, for example, in the case of Coumarine 153 in polar solutions.[24]

Comparison of the SADS λ and μ shows that during the vibrational cooling process the 380 nm band loses a significant part of its intensity. Since no branching occurs in the sequential scheme assumed here, this implies that the transition moment of the excited-state absorption is reduced. This is at odds with expectations within the Born−Oppenheimer approximation where the electronic transition moment is independent of the vibrational content of an electronic state. We therefore have to conclude that the transition is vibronically induced, i.e., instead of vibrational relaxation, we are in fact observing a *vibronic* cooling process.

In previous studies it was concluded that the cooling process can often be divided into two parts.[35] The first part is associated with the energy transfer from the solute to the closest molecules and is determined by solute−solvent interaction. The second, slower, part concerns heat conduction to the outer-sphere solvent molecules and depends largely on the solvent properties. It has been observed that the vibrational cooling rates are proportional to the thermal diffusivity of the solvent if the cooling process is dominated by the second part.[35−37] In line with this observation we observe in the present study that the vibrational cooling rate increases substantially in going from methylcyclohexane (thermal diffusivity 7.60×10^{-8} m^2 s^{-1} [38]) to *n*-dodecane (thermal diffusivity 8.41×10^{-8} m^2 s^{-1} [38]). Since dichloromethane and, in particular, acetonitrile have higher thermal diffusivities,[36] higher vibrational cooling rates would be expected, which might explain at least in part why vibrational cooling was not observed in these two solvents. Predictions using the observed cooling rates of methylcyclohexane and *n*-dodecane show at the same time, however, that the thermal diffusivity argument cannot fully account for the absence of a distinct vibrational cooling process since on this basis vibrational cooling times of about 4 and 2 ps in dichloromethane and acetonitrile, respectively, would have been expected. Since in dichloromethane and acetonitrile solute−solvent interactions are considerably larger than in the apolar solvents, our data suggest that vibrational cooling of DMAN in dichloromethane and acetonitrile is dominated by the solute−solvent interactions responsible for the initial part of vibrational cooling in the model of ref 35.

The last species that can be identified in the present experiments gives rise to the SADS μ in Figure 6. This spectrum agrees very well with the nanosecond transient absorption spectrum determined for the emissive state of DMAN in *n*-hexane.[10] Moreover, the decay times determined here by femtosecond transient absorption are in good agreement with

those obtained by picosecond time-correlated single-photon-counting measurements. We therefore conclude that the species associated with the SADS μ is the relaxed $l\pi^*$ state. This species decays to one or more states that do not further evolve on the time scale of the present experiments. Our previous studies have shown that not only the electronic ground state is involved in this decay, but that also intersystem crossing to the triplet manifold should be taken into account. Interestingly, we find that the lifetime of the relaxed $l\pi^*$ state is rather dependent on the polarity of the solvent. Bagchi, Fleming, and Oxtoby (BFO) have considered the twisting angle dependence of the nonradiative relaxation rate in the dynamics of the twisting processes in triphenylmethane.[39,40] They used a nonlocal sink function as an input function to solve the population density in the excited state from the Smoluchowski diffusion equation while keeping the radiative transition moment unchanged, and showed that this approach leads to a decrease of the lifetime of the excited state with increasing twisting angle. Within this model, the decrease in lifetime of the relaxed $l\pi^*$ state of DMAN would imply that in polar solvents the average twisting angle of the dimethylamino groups is larger than that in apolar solvents.

IV. Conclusions

The energy and geometry relaxation processes occurring after photoexcitation of DMAN in various solvents have been studied with femtosecond fluorescence upconversion and transient absorption techniques. The fluorescence upconversion experiments have shown that after excitation the molecule is subject to an ultrafast process that changes the radiative properties of the state from which emission is monitored considerably. More detailed information could be obtained from the transient absorption experiments. Global fitting of these data to a cascade model has yielded three components for polar solvents (dichloromethane and acetonitrile), and four and five components for the apolar solvents methylcyclohexane and *n*-dodecane, respectively. Analysis of the spectral features present in the SADS has enabled a clear identification of the species associated with each of the components and their primary decay mechanism. We have thus established that upon photoexcitation the ^1L_a state is populated, which undergoes rapid internal conversion to the $l\pi^*$ state. In previous studies it was concluded that this $l\pi^*$ state has significant charge-transfer character and should be subject to major geometry changes driven by the formation of a two-center three-electron bond between the lone pair orbitals of the dimethylamino groups. The evolution of the SADS has in the present study provided direct evidence for such large-amplitude motions, which—in the case of polar solvents—are accompanied by solvent relaxation. In apolar solvents a distinct vibronic cooling process of the geometrically relaxed $l\pi^*$ state could be observed that is absent in polar solvents. The absorption spectrum of the final species that is formed has been shown to be in excellent agreement with previous nanosecond transient absorption studies. Its decay routes involve internal conversion to the ground state and intersystem crossing to the triplet manifold.

Acknowledgment. This work was supported by The Netherlands Organization for Scientific Research (NWO). A.S-H. is grateful to the Royal Dutch Academy of Arts and Sciences (KNAW) and The Netherlands Organization for Scientific Research (NWO) for financial support to participate in the experimental work at the University of Amsterdam. We thank Michiel Groeneveld for experimental assistance.

References and Notes

(1) Alder, R. W.; Bowman, P. S.; Steele, W. R. S.; Winterman, D. R. *Chem. Commun*. **1968**, 723.
(2) Hibbert, F.; Hunte, K. P. P. *J. Chem. Soc., Perkin Trans.* **1983**, *2*, 1895.
(3) Corma, A.; Iborra, S.; Rodriguez, I.; Sanchez, F. *J. Catal.* **2002**, *211*, 208.
(4) Itoh, K.; Oderaotoshi, Y.; Kanemasa, S. *Tetrahedron*: *Asymmetry* **2003**, *14*, 635.
(5) Boussif, O.; F. Lezoualch, F.; Zanta, M. A.; Mergny, M. D.; Scherman, D.; Demeneix, B.; Behr, J. P. *Proc. Natl. Acad. Sci.* **1995**, *92*, 7297.
(6) Behr, J. P. *Chimia* **1997**, *51*, 34.
(7) Hibbert, F. J. *J. Chem. Soc., Perkin. Trans.* **1974**, *2*, 1862.
(8) Einspar, H.; Robert, J. B.; Marsh, R. E.; Roberts, J. D. *Acta Crystallogr*. **1973**, *B29*, 1611.
(9) Szemik-Hojniak, A.; Zwier, J. M.; Buma, W. J.; Bursi, R.; van der Waals, J. H. *J. Am. Chem. Soc.* **1998**, *120*, 4840.
(10) Szemik-Hojniak, A.; Balkowski, G.; Wurpel G. W. H.; Herbich, J.; van der Waals, J. H.; Buma, W. J. *J. Phys. Chem. A* **2004**, *108*, 10623.
(11) Suzuki, K.; Tanabe, H.; Tobita, S.; Shizuka, H. *J. Phys. Chem. A* **1997**, *101*, 4496.
(12) Rotkiewicz, K.; Grellman, K. H.; Grabowski, Z. R. *Chem. Phys. Lett.* **1973**, *19*, 315; **1973**, *21*, 212 (erratum).
(13) Balkowski, G.; Szemik-Hojniak, A.; Deparasinska, I.; Buma, W. J. To be submitted for publication.
(14) Vergeer, F. W.; Kleverlaan, C. J.; Stufkens, D. J. *Inorg. Chim. Acta* **2002**, *327*, 126.
(15) Glasbeek, M.; Zhang, H. *Chem. Rev.* **2004**, *104*, 1929.
(16) Pozharsky, A. F.; Alexandrov, G. G.; Vistorobski, N. V. *Zh. Org. Khim.* **1991**, *27*, 1536.
(17) Because of solubility problems, the signal-to-noise ratio in transient absorption measurements on solutions of DMAN in *n*-hexane was rather low. We therefore employed in these measurements as an alternative solvent methylcyclohexane, which allowed for slightly higher concentrations. For fluorescence upconversion measurements, on the other hand, solutions of DMAN in *n*-hexane were adequate.
(18) Holzwarth, A. R. In *Biophysical Techniques in Photosynthesis*; Amesz, J., Hoff, J., Eds.; Kluwer Academic Publishers: Dordrecht, The Netherlands, 1996; p 76.
(19) van Stokkum, I. H. M.; Larsen, D. S.; van Grondelle, R. *Biochim. Biophys. Acta* **2004**, 262, *1658*.
(20) Analysis of the solvatochromic shift of the emission band within the Onsager cavity approach leads to a dipole moment of the excited state of 3.0 D, which is somewhat larger than the dipole moment of the ground state (1.12 D),[16] but significantly smaller than the dipole moment of the emissive $l\pi^*$ state (9.3 D).[10]
(21) The factor 10 has been calculated for the vertical transition from the ground state. For the calculated equilibrium geometry of the $l\pi^*$ state with perpendicular dimethylamino groups electronic decoupling in the excited state leads to an oscillator strength that a priori is already predicted to be essentially zero.
(22) May, V.; Kühn, O. *Charge and Energy Transfer Dynamics in Molecular Systems*; Wiley-VCH Verlag Berlin GmbH: Berlin, Germany, 2000; p 224.
(23) Wang, H.; Zhang, H.; Rettig, W.; Tolmachev, A. I.; Glasbeek, M. *Phys. Chem. Chem. Phys.* **2004**, 3437.
(24) Horng, M. L.; Gardecki, J. A.; Papazyan, A.; Maroncelli, M. *J. Phys. Chem.* **1995**, *99*, 17311.
(25) Weaver, M. J. *Chem. Rev.* **1992**, *92*, 463.
(26) Kim, H. J.; Hynes, J. T. *J. Photochem. Photobiol. A* **1997**, *105*, 337.
(27) Fonseca, T.; Kim, H. J.; Hynes, J. T. *J. Mol. Liq.* **1994**, *60*, 161.
(28) Fonseca, T.; Kim, H. J.; Hynes, J. T. *J. Photochem. Photobiol. A* **1994**, *82*, 167.
(29) van Veldhoven, E.; Zhang, H.; Rettig, W.; Brown, R. G.; Hepworth, J. D.; Glasbeek, M. *Chem. Phys. Lett.* **2002**, *363*, 189.
(30) Martin, M. M.; Plaza, P.; Changenet-Barret, P. *J. Phys. Chem. A* **2002**, *106*, 2351.
(31) Oxtoby, D. W. *Adv. Chem. Phys.* **1979**, *40*, 1.
(32) Elsaesser, T.; Kaiser, W. *Annu. Rev. Chem. Phys.* **1991**, *42*, 83.
(33) Owrutsky, J. C.; Raftery, D.; Hochstrasser, R. M. *Annu. Rev. Chem. Phys.* **1994**, *45*, 519.
(34) Rückert, I.; Demeter, A.; Morawski, O.; Kühnle, W.; Tauer, E.; Zachariasse, K. A. *J. Phys. Chem. A* **1999**, *103*, 1958.
(35) Iwata, K.; Hamaguchi, H. *J. Phys. Chem. A* **1997**, *101*, 632.
(36) Tan, X.; Gustafson, T. L.; Lefemeux, C.; Burdziński, G.; Buntix, G.; Poizat, O. *J. Phys. Chem. A* **2002**, *106*, 3593.
(37) Benniston, A. C.; Matousek, P.; McCulloch, I. E.; Parker, A. W.; Towrie, M. *J. Phys. Chem. A* **2003**, *107*, 4347.
(38) Sakiadis, B. C.; Coates, J., III. *AIChE J.* **1957**, *3*, 121.
(39) Bagchi, B.; Fleming, G. R.; Oxtoby, D. W. *J. Chem. Phys.* **1983**, *78*, 7375.
(40) Bagchi, B.; Fleming, G. R. *J. Phys. Chem.* **1990**, *9*, 94.